Earth Sciences
2024, Vol. 13, No. 2, pp. 49-57
https://doi.org/10.11648/j.earth.20241302.11

Review Article

The Application of Dual Frequency IP Survey to Identify the Concealed Ore Body in Pilbara Craton, Australia: A Case Study from Calvert Gold Deposit

Zhangle Liu*, Yawen Zheng

Strategic Investment Department, Zijin Mining Investment (Shanghai) CO., LTD., Shanghai, China

Abstract

The Mallina Basin in Western Australia, situated in the central part of the Pilbara Craton which is one of the world's oldest cratons, is a structurally deposited basin subjected to multiple episodes of deformation and magmatic intrusion. The Calvert gold deposit in Mallina Basin is heavily covered by Quaternary, thus, it is hardly to identify any distinct mineralization indicators, and there is no any significant progress in exploration so far. The SQ-3C dual frequency induced polarization facility that is developed by China is introduced to carry out the dual frequency IP survey, the author's team have tested all the types of different rock samples to collect the geophysical parameters in the Calvert area, and the selection of suitable facility and working frequency is based on the geological characters of the Calvert deposit and the geophysical parameters of rocks, and some processes are undertaken to weaken the interference triggered by the electromagnetic coupling, and an IP anomaly zone was delineated. Through the drilling program in the IP anomaly zone, a gold ore body that has the same orientation with the IP anomaly zone was controlled; this result demonstrated the dual frequency IP survey is effective in the local area and provide an efficient technical method for the mineralization prospecting, and this geophysical survey project sets an example for the familiar type of gold deposit in the local area.

Keywords

Dual Frequency Induced Polarization, Australia, Calvert Gold Deposit

1. Introduction

The Pilbara Craton in Western Australia, influenced by multiple tectonic and magmatic events, presents favorable conditions for mineralization [1, 2]. However, most of the Craton is covered by Quaternary, and the surface indications of mineralization are rare, demanding effective exploration methods to detect concealed ore bodies and achieve breakthroughs in resources exploration.

The Dual frequency Induced Polarization Instrument, invented by Academician He Jishan with complete independent intellectual property rights, has been widely applied in various mineral exploration projects in China over the years, and have successfully found various types of concealed metal mineralization in different areas, including epithermal gold mineralization and porphyry copper polymetallic mineralization,
demonstrating excellent exploration results [3-10]. In this

*Corresponding author: liu_zhangle@zijinmining.com (Zhangle Liu)

Received: 18 February 2024; **Accepted:** 8 March 2024; **Published:** 2 April 2024

study, based on the geological, topographical, and physical conditions of the area, a dual frequency induced polarization survey was conducted. One induced polarization anomaly was identified, and through drilling verification, a concealed gold ore body (mineralization) was newly discovered. This indicates the effectiveness of the dual frequency induced polarization in detecting blind ore bodies in the region and showcases its broad application prospects.

2. Geological Background

The Pilbara Craton in Western Australia is one of the world's oldest cratons, characterized by a series of intense tectonic deformations and magmatic activities in the granite-greenstone belts [11-16]. Within its secondary structural units, the Pilbara Craton, primarily composed of the De Grey Group sedimentary rocks and the Whim Creek greenstone belt, has experienced multiple episodes of deformation.

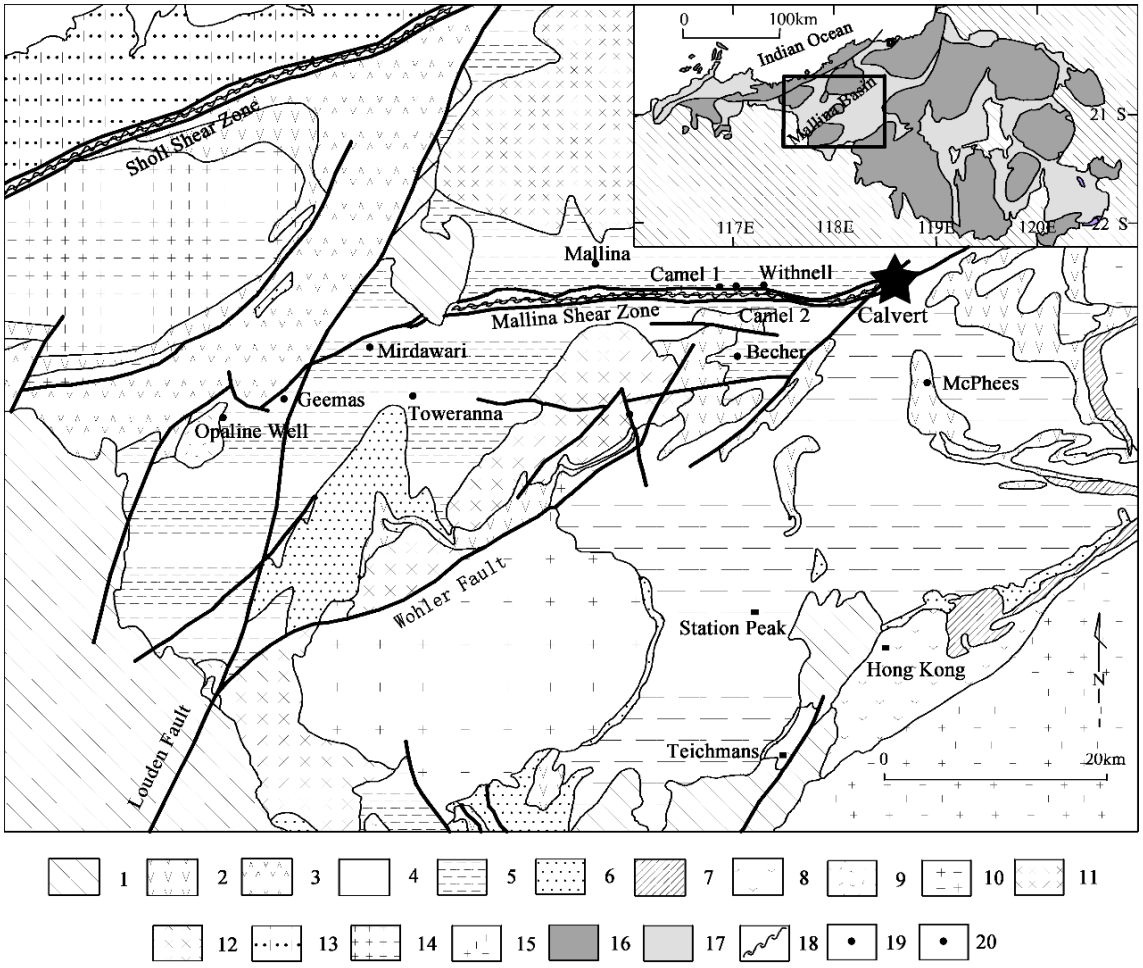

Figure 1. *Geology and Structure of Mallina basin, Central Pilbara (Modified after Bierwirth, 2002).*

1 – Fortescue Group; 2 – Sherlock Intrusion and Millindinna Complex; 3 – Whim Creek Group and Bookingarra Group; 4 – De Grey Group; 5 – Mallina Formation; 6 – Constantine Formation; 7 – Cleaverville Formation; 8 – Pilbara Well Greenstone belt; 9 – Opaline Well Granite; 10 – Satarist Granite; 11 – Portree Granitoid Complex; 12 – Peawah Granodiorite; 13 – Harding Granitoid Complex; 14 – Caines Well Granitoid Complex; 15 – Yule Granitoid Complex; 16 –Granitoid Belt; 17 – Greenstone Belt; 18 – Shear Zone; 19 – Gold deposit

The Mallina Basin, situated in the central part of the Pilbara Craton, is a structurally deposited basin subjected to multiple episodes of deformation and magmatic intrusion. Exposed formations mainly consist of thin-bedded, fine to medium-grained sandstones and shales of the Mallina Formation, overlying coarse-grained feldspar-quartz sandstones and wacke of the Constantine Formation [17]. The Mallina Shear Zone cuts across the Mallina Basin, with its main body showing near-vertical or south-dipping attitudes, displaying signs of southward shear displacement. The swollen part of the Mallina Shear Zone is the primary location for gold mineralization, serving as a hotspot for gold exploration. Various gold deposits of varying scales and types have been discovered within the shear zone and its southern secondary struc-

tural zones. Intrusive rocks primarily include alkaline granites, high-magnesium diorites, and high-potassium diorite granites, with the largest Portree Granite Complex distributed in the northern part of the basin, intruding at 2946 ±6 Ma [18].

The Calvert Gold Deposit is located at the eastern extension of the Mallina Shear Zone intersecting with the Wohler Shear Zone. The terrain is flat, with surface coverings such as aeolian sands, alluvium, colluvium, and calcrete. The geological formations mainly consist of low-grade metamorphic sandstones and shales of the Mallina Group, primarily trending east-west. Secondary structures are predominantly north-south trending, with occasional exposures of small-scale shear structures and near-vertical folds. Magmatic activity in the area is limited, with only a few granite complexes observed.

Previous researchers conducted a series of prospecting works, including surface geology, induced polarization traverses, and soil geochemistry, in the area. Traditional geological work yielded limited success due to scarce outcrops and a lack of prominent mineralization indicators. Induced polarization traverses faced challenges such as strong induction coupling and severe anthropogenic interference, failing to achieve the expected exploration results. Soil geochemistry revealed anomalous Au-As element combinations, suggesting that this anomaly is located at the intersection of two major structural zones, indicating a favorable mineralization background.

3. Physical Characteristics of the Area

The ore bodies mainly consist of sandstone and shale, containing minerals such as pyrite, magnetite, arsenopyrite, quartz, and calcite. The wall rocks primarily comprise conglomerate sandstone and fine sandstone, containing quartz, feldspar, calcite, and biotite. Metal sulfides within the ore bodies are abundant and positively correlated with gold mineralization. Therefore, delineating anomalies induced by metal sulfides through induced polarization surveys can identify significant exploration targets, guiding geological exploration indirectly.

Data collected from various rock samples, including core samples from the surrounding area and surface-collected rock (ore) samples (Table 1), show that the ore-rock amplitude frequency ranges from 2.4% to 8.4%, with an arithmetic mean of 3.9%, and resistivity ranges from 26 to 390 Ω·m, with an average resistivity of 200 Ω·m. The frequency of wall rocks ranges from 0.7% to 3.2%, with an arithmetic mean of 1.93%. The resistivity of sandstone and shale ranges from 15 to 210 Ω·m, with an average resistivity of 95 Ω·m, while the resistivity of granite mixed rock ranges from 165 to 870 Ω·m, with an average resistivity of 470 Ω·m. Overall, there are significant differences in frequency and resistivity between ore-bearing rocks and wall rocks. Ore bodies exhibit high polarization and medium resistivity characteristics, sandstone and shale show low polarization and low resistivity characteristics, while granite mixed rocks display low polarization and high resistivity characteristics. The distinct electrical differences between ore-bearing rocks and wall rocks provide a geophysical basis for electromagnetic surveys [19]. Indirect exploration can be achieved by identifying anomalies reflecting metal sulfides with high polarization and medium resistivity.

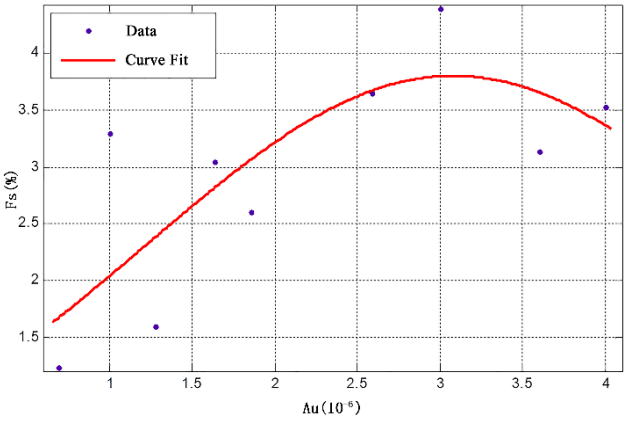

Figure 2. *The amplitude-frequency and gold grade correlation curve.*

Overall, there is a positive correlation between rock sample frequency, gold grade, and pyrite content. The average gold grade of ore samples generally correlates positively with frequency (Figure 2). There is considerable variation in pyrite content between ore and wall rocks, which also correlates positively with gold grade. This suggests that conducting dual frequency induced polarization surveys, verifying geochemical anomalies, and searching for gold mines in the area are feasible, as they have a solid geophysical exploration foundation.

The gold grade of ore samples generally exhibits an approximate positive correlation with frequency. Using the Gaussian curve fitting method, the correlation function between frequency and gold grade is represented by: f(x) = 3.085 * exp{-[(x-3.078)/2.631]2}, where f(x) represents the frequency curve and x represents the gold grade. Generally, the higher the pyrite content, the higher the frequency. However, the frequency is not only related to the amount of pyrite but also to its distribution and ore-bearing lithology. Generally, shale-rich lithologies contain more pyrite in blocky or banded forms, resulting in more pronounced induced polarization characteristics of the ore samples (Table 2).

Table 1. Statistics of physical parameters for rock in exploration area.

Lithology	Samples (Pieces)	Amplitude-Frequency (%)	Amplitude-Frequency Arithmetic mean	Resistivity (Ω·m)	Resistivity Arithmetic mean
Pyrites-quartz sandstone	18	2.4~4.5	3.38	65~390	210
Pyrites shale	20	2.6~8.4	4.42	26~350	192
Siltstone	4	1~1.6	1.33	15~140	83
sale	50	1.3~3.2	2.07	32~210	125
wacke	66	0.7~2.4	1.57	19~120	75
Granite complex	10	1.2~4.1	2.75	165~870	470

Table 2. Statistics of the amplitude-frequency and gold grade.

Ore Type	Lithology Description	Au Grade (ppm)	Amplitude-Frequency (Fs)
Quartz Veins	Pyrites 2%~3%, minor shale		
Quartz Veins	minor shale	0.69	1.23
Quartz Veins	Quartz veins 50%, shale 50%		
Wacke	Quartz veins 5%		
Wacke	Minor shale, Quartz veins 5%	1	3.30
Shale	Few carbonate veins, strongly deformed, pyrites 5%		
Quartz Veins	Quartz veins 95%		
Quartz Veins	Quartz veins 60%, shale 40%	1.28	1.60
Quartz Veins	Minor shale breccia, fine pyrites 5%		
Shale	Quartz veins 60%, fractured	1.86	2.60
Shale	Few carbonate veins, strongly deformed, pyrites 5%	2.59	3.65
Shale	Quartz veins 5%~8%, massive pyrites 5%		
Shale + Quartz Veins	Porphyry breccia in the quartz veins	3	4.40
Shale	Fractured, quartz-carbonate veins 30%, pyrites 1%~2%		
Shale + Quartz Veins	Shale breccia in the quartz veins		
Shale + Quartz Veins	Shale breccia in the quartz veins, pyrites 8%		
Quartz Veins	Quartz veins in the shale, fractured	3.6	3.14
Quartz Veins	Minor pyrophyllitization,		
Shale	Quartz veins 5%		
Siltstone	Shale 30%, quartz veins 15%, siltstone 55%		
Shale+Siltstone	Massive pyrites 7-8%	4	3.53

4. Field Work Methods

The success of geophysical exploration depends heavily on the rational arrangement of field work, the appropriate selection of methods, the establishment of reliable technical parameters, and the implementation of effective interference suppression measures. In the exploration conducted in the Calvert area, Australia, the domestically developed SQ-3C

dual frequency induced polarization instrument was utilized. It employed a dual frequency configuration of 4 Hz and 4/13 Hz, along with a dipole-dipole array. Additionally, a series of measures were taken to reduce electromagnetic coupling effects, ultimately achieving satisfactory exploration results.

4.1. Field Work Arrangement

Geophysical surveys were conducted using a regular grid layout of 100m × 20m (Figure 3), with survey lines perpendicular to the main structural direction. RTK positioning was employed for the survey point locations, with a dipole spacing of 40m and a separation factor of 3. Recording points were positioned at the midpoint between receiving electrodes, and the observed parameters included apparent frequency and apparent resistivity. A total of 11 survey lines and 484 survey points were completed.

4.2. Selection of Work Devices

For electrical surveys, commonly used devices include the gradient array and the dipole-dipole array [20]. While the gradient array is widely used in China due to its convenience in field operations and high measurement efficiency, it also suffers from strong electromagnetic coupling effects in low-resistance areas and complex anomaly shapes when the polarization body is not in the center of the array [21].

In comparison, the dipole-dipole array offers several advantages over the gradient array:

1) The dipole-dipole profile reflects various types and positions of polarization bodies effectively. Different positions of electrodes in the dipole-dipole array facilitate better polarization status, resulting in more distinct polarization anomalies. Profiles with multiple positions and different dipole spacings can be used to draw cross-sectional maps, reflecting the attitude and morphology of polarization bodies more accurately.

2) The dipole-dipole array features completely separate supply and measurement electrodes, offering stronger resistance to inductive coupling effects compared to the gradient array [22, 23].

3) Although anomalies observed with the dipole-dipole array may be more complex than those with the gradient array, the larger data volume and more comprehensive information make it easier to identify induced polarization anomalies [24].

4) The dipole-dipole array exhibits better resolution for steeply dipping polarization bodies compared to the gradient array.

In the early stages, induced polarization surveys were conducted using the gradient array with a 3000m dipole spacing in the Mallina Basin. However, the lengths of the oxidized ore bodies in the area are mostly tens of meters, and the depths of primary ore occurrence are mostly within 300m. The large dipole spacing directly led to a decrease in anomaly resolution, resulting in unsatisfactory exploration results and failed mineral identification during subsequent drilling verification. Reducing the dipole spacing requires additional supply electrodes and a reduction in the number of adjacent survey lines, severely affecting work efficiency. Considering the steep dip of ore bodies and the low surface resistivity of the area (10-40 Ω·m), the dipole-dipole array demonstrates superior resolution for steeply dipping bodies and stronger resistance to low-resistance shielding compared to the gradient array [25]. Therefore, the dipole-dipole array was chosen for this study.

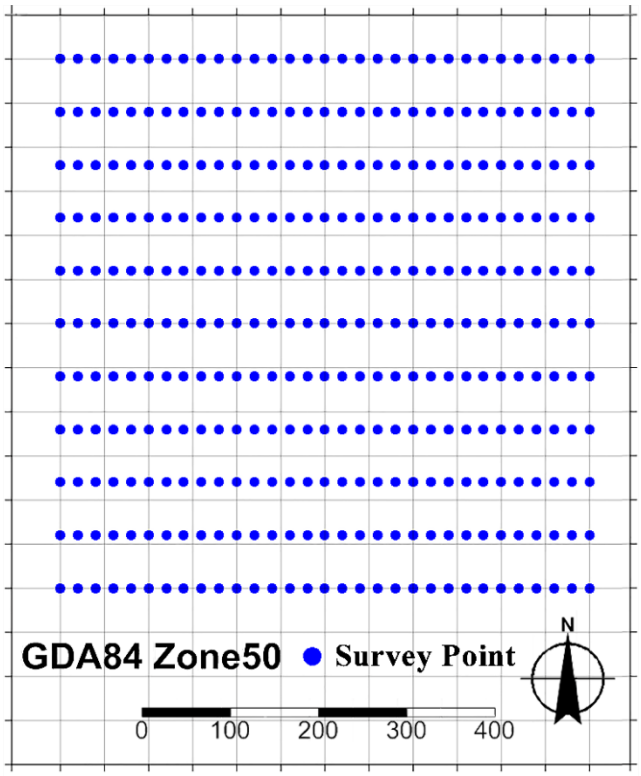

Figure 3. *Dipole-dipole array.*

4.3. Selection of Work Frequency Bands

The main ore-bearing rocks in the area have high sulfide content, often occurring in fine-grained disseminated forms. Selecting the high-frequency band of the dual frequency induced polarization method can yield strong frequency anomalies. To obtain accurate measurements, at least four cycles of the dual frequency signal are generally required, making the high-frequency band more efficient. The maximum operating frequency of the dipole array is calculated using the following formula:

$$f_{max} \leq \rho_s \left(\frac{100}{AB/2}\right)^2 \quad (1)$$

$$f_{max} \leq \rho_s \left(\frac{180}{(n+1)\cdot a}\right)^2 \quad (2)$$

In the equation, a represents the length of the dipole (in meters); n is the isolation factor; ρs denotes the earth resistivity in Ω·m; AB stands for the electrode distance (in meters); f_{max} is the high-frequency of the dual-frequency set (in Hertz). The SQ-3C dual-frequency induced polarization instrument has four operational frequency sets: (1, 1/13 Hz), (2, 2/13 Hz), (4, 4/13 Hz), and (8, 8/13 Hz). Considering the factors mentioned above, based on the calculation results, the dual-frequency 2-point set with a frequency of (4, 4/13 Hz) was ultimately chosen for the survey.

4.4. Measures to Reduce Electromagnetic Coupling Effects

Considering that electromagnetic coupling phenomena are difficult to completely avoid in electrical surveying, in addition to using dipole-dipole arrays with stronger anti-interference capabilities [26], the following measures have been taken to reduce electromagnetic coupling effects:

1) Reduction of Grounding Resistance: Multiple electrodes are connected in parallel to increase the contact area between the soil and electrode rods. Additionally, a large amount of saltwater is poured at the supply electrode positions to decrease grounding resistance, enhance conductivity, reduce energy consumption on grounding resistance, improve the efficiency of power utilization, and ensure the stability of measurement data.

2) Use of More Stable Measurement Electrodes: Copper electrodes with chemically stable properties are selected as measurement electrodes to enhance their stability. During measurements, the electrodes are maintained by sprinkling saltwater to ensure that the inter-electrode grounding resistance is less than 2000 Ω·m, thereby guaranteeing the quality of observation data.

3) Avoidance of Operation During Rainy Days and Crossing of Wires through Water to Reduce Capacitive Coupling Effects: The capacitive coupling effect of the dipole-dipole array is calculated using the following formula [27-32]:

$$\Delta F_s = 2\pi f_c Ran(n+1)(n+2)\ln\left[\frac{(n+1)^2}{n(n+2)}\right] \quad (3)$$

In the equation, ΔFs represents the intensity of the capacitive coupling effect error; n is the isolation factor; a is the length of the dipole, in meters (m); R is the grounding resistance, in ohms (Ω); c is the distributed capacitance of the wire, in picofarads (PF); f is the frequency, in hertz (Hz). The relative error in amplitude-frequency caused by capacitive coupling effects of the four high-frequency bands of the dual frequency induced polarization instrument is calculated separately using the formula. The parameter values are set as follows: c = 20 pF, R = 1000 Ω, a = 100 m, and n = 3. The results of the calculation of the relative error in amplitude-frequency caused by capacitive coupling effects are shown in Table 2.

The calculation results in Table 2 indicate that the capacitive coupling effect is generally insignificant. However, when the wires are submerged in water or laid on relatively damp ground, the distributed capacitance c can be tens of times higher than that in dry conditions, resulting in a significant increase in the capacitive coupling effect. Therefore, it is necessary to avoid working in wet conditions after rain to minimize the effects of capacitive coupling during fieldwork.

Despite the possibility of electromagnetic coupling interference in the area, practical experience has shown that by implementing the aforementioned three measures, the impact has been minimized within a controllable range, ensuring the quality of measurement data.

5. Interpretation of Results and Drilling Verification

The dual frequency induced polarization survey revealed prominent apparent frequency anomalies (Figure 4), and drilling verification confirmed the presence of a significant industrial ore body. This demonstrates that the dual frequency induced polarization method is an effective and feasible means of identifying gold blind ore bodies associated with sulfides in the area, providing substantial technical support for mineral exploration breakthroughs in the region.

5.1. Electrokinetic Anomaly Characteristics

The anomalies, concentrated along a north-south trend in the central part of the survey area, exhibit high intensities with apparent frequency (Fs) values close to 4%. Anomalous zones in the southwest of the area remain unclosed, suggesting the possible extension of polarized bodies in that direction. Defining anomalies with an apparent frequency value of 3.1%, a closed anomalous zone, designated as A1, measuring 300 meters long in the north-south direction and 250 meters wide in the east-west direction, corresponding to a mid-resistance anomaly, was delineated. While magmatic intrusions are rare at the surface, the high-resistance anomalies observed in the northwest (Figure 4b) may reflect deep-seated rock or intrusion bodies. The widespread mid-to-low resistance anomalies reflect the predominance of turbidite deposits composed mainly of sandstone, shale, and siltstone in the geological strata. The north-south trending gradient of resistance anomalies suggests possible shear effects in the strata, indicating the presence of secondary structures. From the analysis of resistance anomalies, it cannot be ruled out that mineralized bodies in this area may be closely related to magmatic activity. The Calvert area is located at the intersection of two regional faults, with no apparent signs of magmatic activity at the surface. Similar to the Opaline Well deposit (Figure 1), a fault-controlled gold deposit located at the intersection of regional faults in the Mallina Basin, the structural characteristics of the Calvert area are comparable. Based on apparent frequency anomaly A1, combined with the results of physical property measurements, it is speculated that a shallow-level

gold mineralized body may exist in the Calvert area. The A1 anomaly zone identified during this geophysical survey will be prioritized as a key exploration target area in the subsequent exploration work, with drilling verification work being the primary focus.

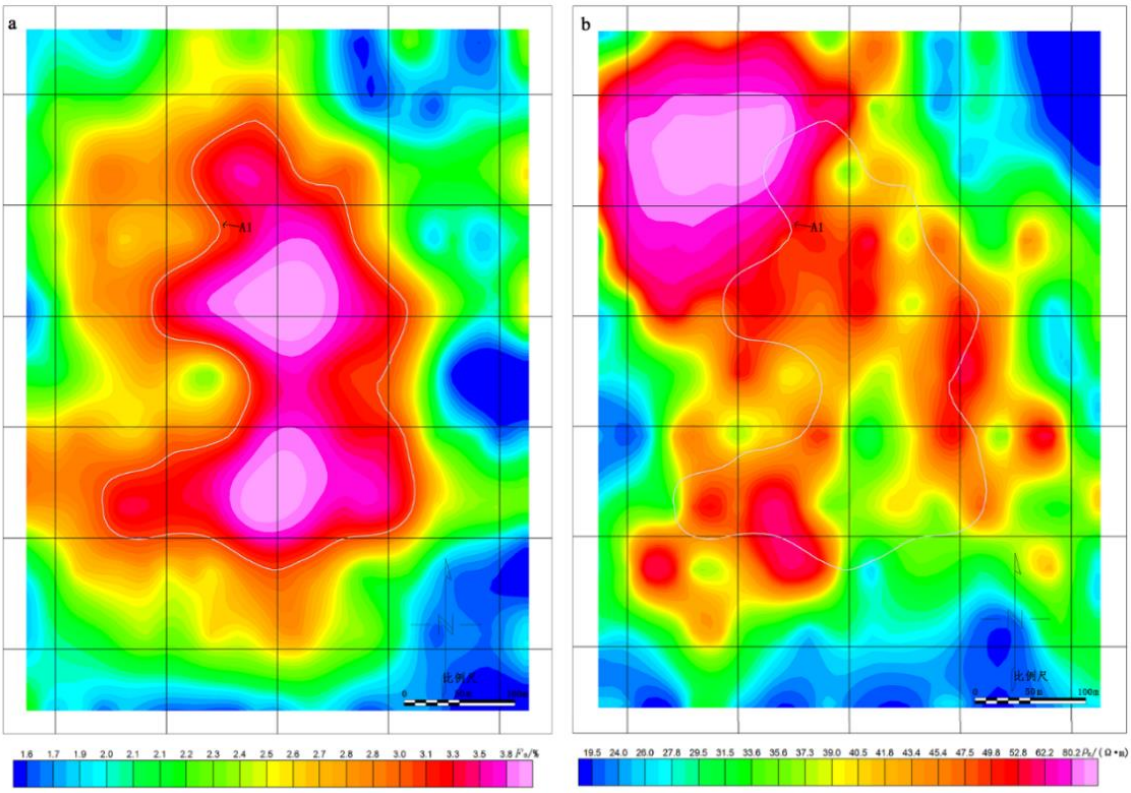

Figure 4. *Dual frequency IP apparent amplitude frequency (a) and resistivity plane (b).*

5.2. Drilling Verification Results

Based on the distribution range, scale, and intensity of the geophysical anomaly target area A1, the first batch of five shallow drilling verification projects were set up along the A1 anomaly zone within the area. Drilling was conducted at depths of up to 75 meters along the 100-meter grid lines. All five boreholes encountered mineralization (Figure 5). Subsequently, a second batch of denser control and peripheral exploration drilling projects were initiated (Figure 5) to explore the continuity and extension of the ore body. The results indicated that the vast majority of mineralized boreholes were located within the A1 anomaly zone, with only two boreholes outside the anomaly zone boundaries encountering mineralization. The drilling results confirmed the presence of a north-south trending gold industrial ore body within the area, which is stratiform in nature, with an average grade of 1.2 g/t, an average thickness of 24.5 meters, and dip angles ranging from 35 °to 43 °. The ore body exhibits a high content of pyrite (>1%) while the surrounding rock content drops to background level. The extent of the ore body aligns closely with the A1 anomaly zone.

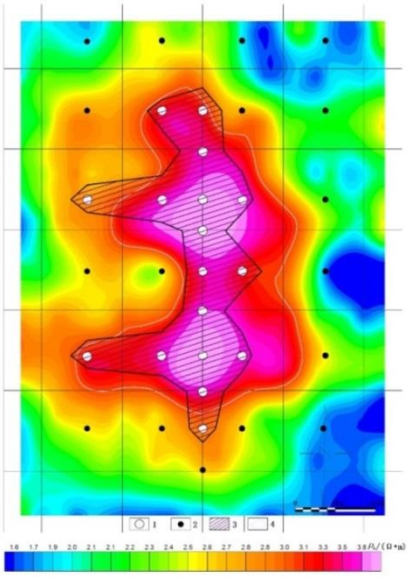

Figure 5. *The geophysical anomaly and ore body and drill holes layout.*

1 Drill holes with intersection; 2 Drill holes without intersection; 3 Mineralization boundary; 4 Anomaly zone A1

6. Conclusion

1) There are significant electrical differences between the ore and wall rocks in the Calvert area, and indirect exploration can be achieved by delineating induced polarization anomalies. The geological prerequisites for conducting induced polarization measurements exist within the area.
2) In areas where magmatic activity is not significant, gold mineralization associated with metallic sulfides tends to occur in areas of structural intersection enlargement. The dual frequency induced polarization method can be used in such areas to indirectly explore gold mineralization using anomalies in apparent frequency and resistivity.
3) The Pilbara Craton region exhibits relatively high consistency in topography and geomorphology. The effective selection of geophysical equipment, working frequency groups, and measures to reduce electromagnetic coupling interference in this work are tailored to local conditions and have achieved good results. This work has important implications for conducting similar induced polarization surveys in areas with high sulfide content in the Pilbara Craton region.
4) The verification results of drilling projects directly confirm the feasibility of the dual frequency induced polarization method in locating blind ore bodies in areas with severe surface cover in the Pilbara Craton region of Australia. Introducing newly developed geophysical methods and instruments from China into a mining powerhouse country opens up new possibilities for future exploration work in the region, promising to change the landscape of exploration activities in the area.

Abbreviations

IP: Induced Polarization
PPM: Parts Per Million
FS: Amplitude-Frequency

Conflicts of Interest

The authors declare no conflicts of interest.

References

[1] Huston D L, Smithies R H, Sun S-S. Correlation of the Archaean Mallina-Whim Creek Basin: Implications for base-metal potential of the central part of the Pilbara granite-greenstone terrane. Australian Journal of Earth Sciences, 2001, 47(2): 217-230. https://doi.org/10.1046/j.1440-0952.2000.00775.x

[2] Jaques A L, Subhash Jaireth, John Walshe. Mineral systems of Australia: An overview of resources settings and processes. Australian Journal of Earth Sciences, 2002, 49(4): 623-660. https://doi.org/10.1046/j.1440-0952.2002.00946.x

[3] Liu J X, Liu C M, Tong T G, Liu H F. The application of the dual frequency induced polarization method in a copper and polymetallic ore deposit in Tibet. Geology and Exploration, 2004, 40(2): 59-61. https://doi.org/10.3969/j.issn.0495-5331.2004.02.013

[4] Zhou Y M. Application effects of geophysical prospecting method for hidden deposits in the northeastern yunnan. Geology and Exploration, 2006, 42(3): 81-85. https://doi.org/10.3969/j.issn.0495-5331.2006.03.016

[5] Wu W, Zhang B L, Liang G H, Li Z Y, Shen X L, Qi M. Application of dual—frequency IP method in metal ore prediction in two types of typical overburden areas in Western China. Geology and Exploration, 2009, 45(6): 669-675. https://kns.cnki.net/kcms2/article/abstract?v=HboJJBuTKtQOgCUor-uCBj8m3R0pFKlwKZE-_Xbi3jpA7LDXiAJEmoBojTc4wazTkmRJKcNRX66ootcWZ0L7IB6wcsqbQE6OupGZkmLch6cT-WMmWxHVALsVL4hQCRZgBgmbXN8ZgV6s=&uniplatform=NZKPT&language=CHS

[6] Dai Q W, Zhang B, Feng D S, Chen D P, Yu K. Integrated detection of leakage paths in reservoirs by the pseudorandom flow—field method and dual frequency induced polarization method. Progress in Geophysics, 2010, 25(4): 1453-1458. https://doi.org/10.3969/j.issn.1004-2903.2010.04.037

[7] Yang L G, Liu J S, Yin L J, Liu W M, Liu W H, Guo J. Application of the dual— frequency IP method to rapid prospecting of mineral resources in the Lizi area of Gansu Province. Geology and Exploration, 2013, 49(2): 330-336. http://www.dzykt.com/dzyktcn/ch/reader/view_abstract.aspx?file_no=20130215&flag=1

[8] Yang Z W, Yan J Y, Chen X B. The application of spectral induced polarization in Shaxi porphyry copper in Anhui Province. Progress in Geophysics, 2013, 28(4): 2014-2023. https://doi.org/10.6038/pg20130445

[9] Li H W, Bai J, Huang X. Application of electrical survey on a porphyry copper deposit exploration area of Gongbogyamda County, Tibet. Geoscience, 2014, 28(4): 850-858. https://doi.org/10.3969/j.issn.1000-8527.2014.04.024

[10] Li J L. Application of the down—hole IP method to a general survey in the Jinya gold deposit. Geology and Exploration, 2016, 52(5): 924-930. https://d.wanfangdata.com.cn/periodical/ChlQZXJpb2RpY2FsQ0hJTmV3UzIwMjMxMjI2Eg5kenlrdDIwMTYwNTAxMxoIZTNreGljcGw%3D

[11] Huston D L, Blewett R S. Lode Gold and Epithermal Deposits of the Mallina Basin, North Pilbara Terrain, Western Australia. Economic Geology, 2002. 97, 801-818. https://doi.org/10.2113/gsecongeo.97.4.801

[12] Barley M E. The tectonic and metallogenic evolution of the Pilbara Craton: preface. Precambrian Research, 1998. 88: 1-2.

[13] Collins W J, Van Kranendonk M J, Teyssier C. Partial convective overturn of Archaean crust in the east Pilbara Craton, Western Australia: Driving mechanisms and tectonic implications. Journal of Structural Geology, 1998. 20(9): 1405-1424. https://doi.org/10.1016/S0191-8141(98)00073-X

[14] Nelson D R, Trendall A F, Altermann W. Chronological correlations between the Pilbara and Kaapvaal cratons. Precambrian Research, 1999. 97(s3-4): 165-189. https://doi.org/10.1016/S0301-9268(99)00031-5

[15] Hickman H. Two contrasting granite-greenstone terranes in the Pilbara Craton, Australia: Evidence for vertical and horizontal tectonic regimes prior to 2900 Ma. Precambrian Research, 2004.131(3): 153-172. https://doi.org/10.1016/J.PRECAMRES.2003.12.009

[16] Blewett R S. Archaean tectonic processes: a case for horizontal shortening in the North Pilbara Granite-Greenstone Terrane, Western Australia. Precambrian Research, 2002. 113: 87-120. https://doi.org/10.1016/J.PRECAMRES.2003.12.009

[17] Smithies R H, Nelson D R, Pike G. Development of the Archaean Mallina Basina, Plibara Craton, northwestern Australia; a study of detrital and inherited zircon ages. Sedimentary Geology, 2001. 141-142: 79-94. https://doi.org/10.1016/S0037-0738(01)00069-0

[18] Smithies R H, Champion D C, Sun S S. Evidence for Early LREE-enriched Mantle Source Regions: Diverse Magmas from the c. 3.0Ga Mallina Basin, Pilbara Craton, NW Australia. Journal of Petrology, 2004. 45: 1515-1537. https://doi.org/10.1093/PETROLOGY/EGH014

[19] Cui Y A, Ji T X, Li X Y, Zhu X X. Inversion of multi—anomalies in resistivity profiling based on particle swarm optimization. Progress in Geophysics, 2013, 28(4): 2164-2170. https://doi.org/10.6038/pg20130462

[20] Bai Y C, Zuo H, Luo W B. Several technique problems in dual-frequency IP method used in reconnaissance survey. Mineral Resources and Geology, 2003, 17(S1): 451-454. https://doi.org/10.3969/j.issn.1001-5663.2003.z1.054

[21] Wang H Y, Li T. The application of dual frequency IP method to the exploration of mineral resources in Western Australia. Geophysical and Geochemical Exploration. 2016, 40(5): 923-928. https://doi.org/10.11720/wtyht.2016.5.13

[22] Zhan K, Zhu B Q. Electromagnetic coupling of ladder device in the frequency domain of uniform earth. Geophysical and Geochemical Exploration, 1981, 5(1): 11-16. https://www.wutanyuhuatan.com/CN/article/downloadArticleFile.do?attachType=PDF&id=3233

[23] Xiong B, Yu Y C. Numerical calculation and analysis of induction coupling of double frequency IP method. Computing Techniques for Geophysical and Geochemical Exploration, 2009, 31(1): 30-35. https://doi.org/10.3969/j.issn.1001-1749.200

[24] Qiang J K, He J S. Algorithm of forward and inversion of dual—frequency induced polarization method on elliptical sphere. J. Cent. South Univ. (Science and Technology), 2007, 38(6): 1199-1205. https://doi.org/10.3969/j.issn.1672-7207.2007.06.032

[25] Wynn J C, Zong K L. Electromagnetic coupling. Geophysical Prospecting, 1977, 25(1): 29-51. https://doi.org/10.1111/j.1365-2478.1977.tb01151.x

[26] Wang L, Yang W, Zou L Z. On Dual— Frequency IP Abnormal Observation in the Intermediate Gradient. Chinese Journal of Engineering Geophysics, 2009, 6(5): 607-611. https://doi.org/10.3969/j.issn.1672-7940.2009.05.016.

[27] Wang L, Zou L Z, Yang W. An Exploration Case of IP Gradient Method in a Lead-Zinc Ore in the Middle of Dongchuan. Chinese Journal of Engineering Geophysics. 2009, v. 6(06): 708-711. https://doi.org/0.3969/j.issn.1672-7940.2009.06.007

[28] Yu L, Ma H L, Li D. A Study of Water Tank Modeling Based on Dual-frequency IP Method. Chinese Journal of Engineering Geophysics. 2010, v. 7(03): 307-312. https://doi.org/10.3969/j.issn.1672-7940.2010.03.008

[29] Liu J X, Gong L, Liu H F. Application of Dual-frequency Induced Polarization Method for Water Exploration in Gobi, Xinjiang. Chinese Journal of Engineering Geophysics. 2013, v. 10(06): 745-751. https://doi.org/10.3969/j.issn.1672-7940.2013.06.001

[30] Zhou W, Yuan J L, Ran Z Y. The Application of Dual-frequency IP Method to Surveying Polymetallic Ore Deposits in Yueqiacuo Area of Tibet. Chinese Journal of Engineering Geophysics. 2014, v. 11(01): 12-17. https://doi.org/10.3969/j.issn.1672-7940.2014.01.003

[31] Huang X C, Lin R S, Yu J J. The Application of Dual-frequency IP Sounding to One Geothermal Exploration. Chinese Journal of Engineering Geophysics. 2015, v. 12(04): 455-458. https://doi.org/10.3969/j.issn.1672-7940.2015.04.006

[32] Zhang D S, Yang B N, He S. Application Research of Geophysical Method on Lead-zinc Mine Area in Panshi, Songtao County. Chinese Journal of Engineering Geophysics. 2020, v. 17(04): 447-456. https://doi.org/10.3969/j.issn.1672-7940.2020.04.009